Journal of Food Chemistry & Nanotechnology

http://dx.doi.org/10.17756/jfcn.2016-022

Research Article

Open Access

Polydiacetylene Vesicles for Detecting Surfactants: Understanding the Driven Forces of Polydiacetylene-Surfactant Interaction

Ana Clarissa S. Pires[1*], Nilda de Fátima F. Soares[1*], Luis Henrique M. da Silva[2], Maria do Carmo H. da Silva[2], Jaqueline de P. Rezende[1] and Geany Peruch Camilloto[3]

[1]Departamento de Tecnologia de Alimentos, Centro de Ciências Exatas e Tecnológicas, Universidade Federal de Viçosa, Av. P.H. Rolfs, s/n, Viçosa, MG, 36570-000, Brazil
[2]Departamento de Química, Centro de Ciências Exatas e Tecnológicas, Universidade Federal de Viçosa, Av. P.H. Rolfs, s/n, Viçosa, MG, 36570-000, Brazil
[3]Departamento de Tecnologia, Universidade Estadual de Feira de Santana, BR 116, km 3, s/n, Feira de Santana, BA, 44031-580, Brazil

[*]Correspondence to:
Ana Clarissa S. Pires
Departamento de Tecnologia de Alimentos
Centro de Ciências Exatas e Tecnológicas
Universidade Federal de Viçosa, Av. P.H. Rolfs
s/n, Viçosa, MG, 36570-000, Brazil
Tel: +55 31 38991625
Fax: +55 31 38992208
E-mail: ana.pires@ufv.br

Nilda de Fátima F. Soares
Departamento de Tecnologia de Alimentos
Centro de Ciências Exatas e Tecnológicas
Universidade Federal de Viçosa, Av. P.H. Rolfs
s/n, Viçosa, MG, 36570-000, Brazil
Tel: + 55 31 38991624
Fax: +55 31 38992208
E-mail: nfsoares@ufv.br

Received: May 23, 2016
Accepted: August 08, 2016
Published: August 10, 2016

Citation: Pires ACS, Soares NFF, da Silva LHM, da Silva MCH, Rezende JP, et al. 2016. Polydiacetylene Vesicles for Detecting Surfactants: Understanding the Driven Forces of Polydiacetylene-Surfactant Interaction. *J Food Chem Nanotechnol* 2(3): 138-146.

Published by United Scientific Group

Abstract

Surfactants are widely used by food industry thus its discharge is an environmental concern; and development of Polydiacetylene (PDA)-based sensors may detect these molecules. However, to improve the sensor efficiency is necessary to understand interactions between PDA vesicles and surfactants. In this work, we purpose to investigate the interactions between surfactants and PDA vesicles as well as between surfactants and PDA + cholesterol (CHO) + sphingomyelin (SPH) vesicles dispersed in water. The addition of a cationic surfactant, hexadecyltrimethylammonium bromide (CTAB), induced a blue-to-red spectrophotometric transition in both structures; however, the addition of the anionic compounds, sodium dodecyl sulfate (NaDS) and lithium dodecyl sulfate (LiDS) did not change the vesicle color. The addition of the cationic surfactant increased the hydrodynamic radium (R_h) of the PDA vesicles (from 39.82 ± 3 nm to 96.85 ± 3 nm) and the PDA/CHO/SHP vesicles (from 160.89 ± 3 nm to 219.84 ± 3 nm). The presence of NaDS and LiDS also increased the size of the PDA vesicles (to 43.50 ± 3 nm and 43.75 ± 3 nm, respectively) and the PDA/CHO/SPH vesicles (to 201.91 ± 3 nm and 210.24 ± 3 nm, respectively). The interaction energies between the cationic surfactant and PDA and PDA/CHO/SPH were different; however, both were entropically driven. PDA vesicles show potential to be used as sensors for cationic surfactants detection.

Keywords

10,12-pentacosadiynoic acid, Cholesterol, Sphingomyelin, Surfactants, Enthalpy

Introduction

Surfactants are widely applied to clean surfaces of equipment used in food industry [1]. In addition, it has been recognized that some surfactants, such as sodium dodecyl sulfate (SDS), improve microbial efficacy of antimicrobials, because they enhance the membrane penetration of other antimicrobials compounds present in formulations [2]. Thus, the extensive use of surfactants by food industry and also by other segments result in massive discharge of these molecules into the environment leading to an environmental concern [3]. Therefore, there is an increasing interest in developing simple, fast and low cost techniques to detect these molecules.

As is well known, polydiacetylene vesicle building by self-organized diacetylene monomers and then polymerized by UV light could be used as nanosensors due to its molecules undergo spectrophotometric transitions in

response to different stimuli, such as temperature change [4-6], pH [5, 7, 8], mechanical stress [9, 10], solvents [5, 11, 12], and interaction with other molecules, such as surfactants [13-19].

It is well recognized that PDA optical absorption occurs via π-π^* electronic transitions within a linear π-conjugated polymer backbone, which has two spectroscopically distinct phases. The blue and red forms result from absorption peaks at approximately 650 and 540 nm, respectively [20, 21]. In order to optimize the PDA vesicle application as surfactant nanosensors is fundamental to know the driving force for vesicle-surfactant interaction. However, the mechanism of the colorimetric transition caused by the solute-vesicle molecular interaction is not fully understood.

In a previous study, we verified that the mechanism of the blue-to-red transitions depends on the vesicle-organic solvent interaction. As we demonstrated, the enthalpy changes associated with the PDA colorimetric transition are a result of conformational changes associated with the rotation of the functional group around the carbon-carbon bond present in polydiacetylene chains [12, 22].

Amphiphilic molecules are able to induce PDA colorimetric transition. Su et al. [15] have evaluated the colorimetric response of PDA molecules in the presence of different surfactants; they proposed that the insertion of the CTAB alkyl chain into the hydrophobic domain perturbs the conformation of the conjugated polymer backbone and induces a color change in the polydiacetylene vesicles. In another work Su et al. [17], the same authors investigated the influence of amphiphilic molecules on the colorimetric transition of PDA molecules that were incorporated into a phospholipid vesicle (Dimyristoyl phosphatidylcholine, DMPC). They found that an increase in DMPC content enhanced the surfactant's interaction with the mixed vesicles because DMPC promoted the insertion of surfactant hydrophobic chains into the membrane lipids. However, to the best of our knowledge, no experimental evidence of this surfactant insertion into the vesicle hydrophobic core has been reported. Apart from the efforts in developing new sensors for detecting molecules, such as surfactants, another important aspect is the knowledge about the detection mechanisms, because it certainly improves the sensor efficiency.

Thus, to contribute to understanding the mechanism of surfactant-vesicle interaction, and therefore optimizing the development of efficient sensors for cationic surfactants, we measured the enthalpies of the vesicle-surfactant interactions and correlated this energy with the spectrophotometric transitions of 10,12-pentacosadiynoic acid (PDA) and PDA + cholesterol (CHO)+sphingomyelin (SPH) vesicles induced by cationic (hexadecyltrimethylammonium bromide, CTAB) and anionic (sodium dodecyl sulfate, NaDS, and lithium dodecyl sulfate, LiDS) surfactants.

Experimental

Vesicle preparation

The PDA and PDA/CHO/SPH vesicles were prepared as described elsewhere [12, 23-25]. Briefly, to obtain PDA vesicles, the PDA monomer (10,12-pentacosadiynoic acid, 97% w/w, Sigma®) was dissolved in $CHCl_3$ (98% w/w, Sigma®), which was removed by a stream of N_2 gas to promote the formation of a PDA film on the glass surface. Deionized water was added until the PDA concentration reached 1 mM. The resulting suspension was sonicated (SoniTech, 300 W, 40 kHz) at 70 °C until a clear solution was obtained, which was immediately filtered using a 0.45 µm PVDF filter (Milipore®).

To produce PDA/CHO/SPH vesicles, PDA monomer was dissolved in 2 mL of dimethyl sulfoxide (99% w/w, Merck®), and CHO (99% w/w, Sigma®) and SPH (from chicken egg yolk, 98% w/w, Fluka®) were dissolved in 2 mL of $CHCl_3$ (98% w/w, Sigma®), which was removed by a stream of N_2 gas. The PDA was added to the CHO and SPH and maintained at 80 °C for 15 min. Deionized water was added until the PDA, CHO and SPH concentrations reached 1 mM. The resulting suspension was sonicated at 70 °C until a clear solution was obtained, which was immediately filtered using a 0.45 µm PVDF filter.

In order to correct the PDA concentration in both vesicles after filtration step, we performed an analytical curve from absorbance *versus* PDA concentration. To obtain this curve, vesicles were prepared with different PDA concentration and lyophilized. The ratio between the lyophilized mass and PDA molar mass provided the final PDA concentration in vesicles. Plotting absorbance *versus* PDA concentration, the molar absorption coefficient of PDA was determined and it was used to calculate PDA concentration in PDA/CHO/SPH vesicle. The final and real PDA concentrations in both systems were 0.084 and 0.087 mM for PDA and PDA/CHO/SPH vesicles, respectively.

Both vesicular suspensions were stored at 4 °C overnight to promote lipid and PDA crystallization. Photopolymerization of vesicles was achieved by exposure to UV radiation (254 nm) for 10 minutes, which resulted in blue-colored PDA vesicles.

Dynamic light scattering

The vesicle samples were diluted by a factor of 20 with deionized water, filtered through a 0.45 µm PVDF filter (Milipore®) and stored in hermetic vials. The size of the vesicles was determined using a Nanophox DLS in autocorrelation mode equipped with a 632.8 nm HeNe laser from Sympatec (Clausthal-Zellerfeld, Germany). The zeta potential of vesicles were measured at 25 °C, with a Zetasizer nano ZS90 (Malvern, UK). Each experiment was repeated 3 times, and each result was presented as the average of 10 measurements.

Colorimetric response (CR)

The effect of different surfactants on the PDA and PDA/CHO/SPH vesicles was analyzed by adding 42 µL of surfactant solution (CTAB, NaDS or LiDS) to 3.0 mL of the vesicle suspension in 3.0 µL intervals. The UV–visible spectra were measured between 400 and 700 nm (Shimadzu UV-2550) at 298 K. To quantify the extent of the PDA molecule blue-to-red color transition, the CR (%) was calculated using the equation proposed by Charych et al. [26] (Equation 1).

$$CR = \left[\frac{\left(\frac{A_{blue}}{A_{blue} + A_{red}} \right)_b - \left(\frac{A_{blue}}{A_{blue} + A_{red}} \right)_a}{\left(\frac{A_{blue}}{A_{blue} + A_{red}} \right)_b} \right] x100 \quad \ldots\ldots\ldots\ldots (1)$$

Where A is the absorbance of the blue (~ 650 nm) and red (~ 540 nm) bands measured by UV-visible spectroscopy. The terms "blue" and "red" refer to the appearance of the solutions, and the indices "b" and "a" represent the absorbance before and after exposure to the surfactant stimuli.

Isothermal titration calorimetry

A CSC model 4200 isothermal titration microcalorimeter (ITC) in titration mode was used for the analyses. The mixture vessel consisted of 1.82 mL stainless steel cells surrounded by a thermostatic bath. To measure the enthalpy change (ΔH), 1.82 mL of the vesicular suspension was added to the sample and reference cells, which were agitated at 300 rpm. When thermal equilibrium was reached between the cells and the bath, 1 μL of each surfactant solution was titrated into the vesicle suspension in the sample cell at 120 minute intervals using a Hamilton micro-syringe. All measurements were performed in triplicate, and the standard deviation was approximately 0.5%.

The whole calorimetric procedure was chemically and electrically calibrated to the heat of protonation of (Tris(hydroxymethyl)aminomethane) and the joule effect, as recommended by Mageste et al. [27].

Results and Discussion

Figure 1 shows the electronic spectra of the PDA and the PDA/CHO/SPH vesicular suspensions at the same PDA concentration and in the blue structural form. Both suspensions exhibit a maximum absorption peak at 640 nm with a shoulder at 590 nm. These results indicate that even though CHO and SPH were incorporated into the vesicles, they did not affect the polymerization and the electronic transition, as Boullanger et al. [28], Su et al. [15] and Sun et al. [29] have also observed. Lipid molecules form microdomains inside the PDA matrix; therefore, their incorporation does not affect the PDA electronic transition responsible for the blue color [30].

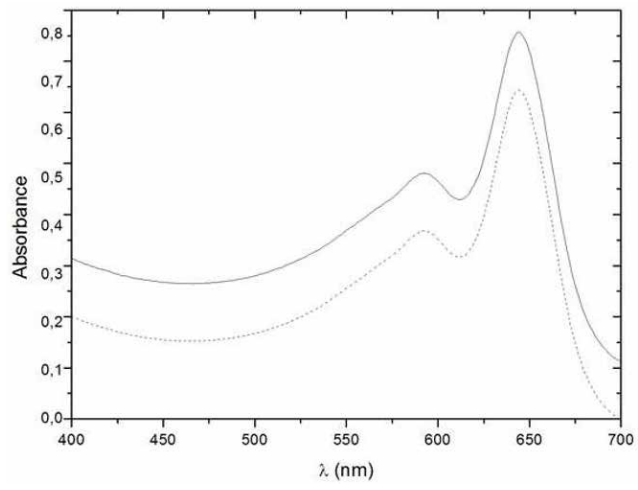

Figure 1: Electronic spectra of the (---) PDA and the (—) PDA/CHO/SPH vesicular suspensions at the same PDA concentration (1.0 mM) and in the blue structural form.

The spectra also show that the presence of CHO and SPH molecules promoted the formation of vesicles with absorption intensity greater than nano-aggregates containing only PDA. Such behavior is related to higher polymerization yield of PDA into PDA/CHO/SPH vesicles compared with PDA vesicles.

Typical changes in the electronic spectra of PDA macromolecules after the addition of the cationic surfactant are shown in Figure 2. After the addition of 42 μL of the CTAB aqueous solution at critical micellar concentration (c.m.c. = 9.2×10^{-2} mol.L^{-1}) into 3.0 mL of the 1.0 mM suspension of PDA vesicles, achieving 3.8×10^{-5} mol.L^{-1} CTAB final concentration, the peak intensity at 640 nm became zero, and a new peak appeared at 540 nm. This behavior indicated that the concentration of PDA molecules with structure that absorbs at 640 nm decreased and the number of PDA molecules with conformation that absorb at 540 nm increased. However, when the aqueous solutions of anionic surfactants NaDS or LiDS were added to the vesicular suspension, no color transition was observed, suggesting no vesicle-anionic surfactant interaction. As the PDA vesicle surface are negatively charged (–20.10 ± 0.15 and –26.50 ± 0.43 mV, for PDA and PDA/CHO/SPH, respectively) due the carboxylic group ionization, probably the absence of vesicle-anionic surfactant interaction is due to an electrostatic repulsion contribution to dodecyl sulfate (DS)-PDA interaction. The more negative zeta potential observed for vesicles containing CHO and SPH is due to the higher stabilization of carboxylic groups of PDA promoted by PDA-CHO and/or PDA-SPH interactions. This result also suggest that both co-solutes are present on vesicle surface since a surface property (zeta potential) was changed.

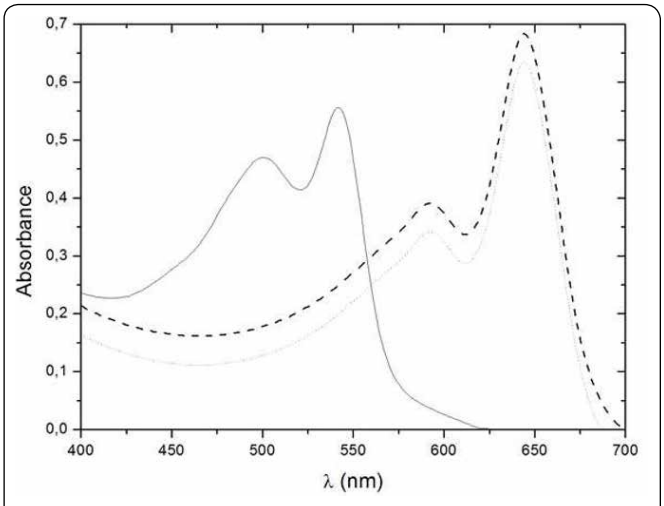

Figure 2: Effect of surfactants on the electronic spectra of PDA macromolecules: (—) cationic surfactant CTAB (3.8×10^{-5} mol.L^{-1}) and anionic surfactants: (---) NaDS (3.6×10^{-4} mol.L^{-1}) and (···) LiDS (3.6×10^{-4} mol.L^{-1}).

The colorimetric response (CR) of the PDA and PDA/CHO/SPH vesicles as a function of CTAB, NaDS or LiDS

concentration are presented in Figures 3 and 4, respectively. The CR value is a quantitative measurement of the percentage of blue PDA molecules converted into red PDA molecules [31]. The presence of the cationic amphiphilic molecules (CTAB) induced the spectrophotometric transition in both vesicle structures. The colorimetric response induced by CTAB was more pronounced in PDA vesicles than in PDA/CHO/SPH nanostructures. Approximately four times more CTAB was required to promote the same CR (40%) in the PDA/CHO/SPH system compared to PDA vesicle. This behavior is explained by vesicle rigidity caused due to interaction between CHO and SPH molecules [32] and between them and with PDA via hydrogen bonding [33]; thus PDA/CHO/SPH were more thermodynamically stable structures [34] than pure PDA nanostructure.

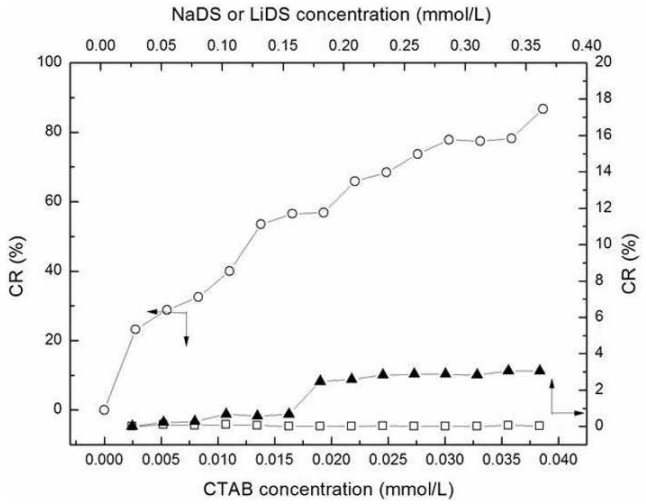

Figure 3: Colorimetric response (CR) of PDA vesicles as a function of (○) CTAB, (▲) NaDS and (□) LiDS final concentration, at 25 °C.

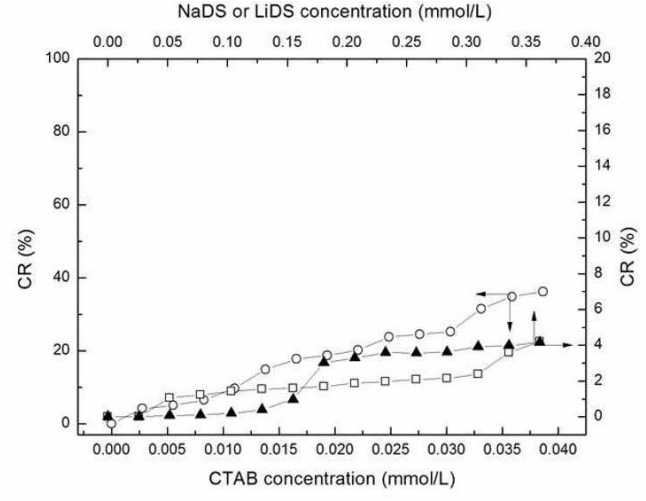

Figure 4: Colorimetric response (CR) of PDA/CHO/SPH vesicles as a function of (○) CTAB, (▲) NaDS and (□) LiDS final concentration, at 25 °C.

Su et al. [15, 17] have also studied the interaction between amphiphilic molecules and polydiacetylene vesicles incorporated with Dimyristoyl phosphatidylcholine (DMPC) and found similar results. CTAB induced a blue-to-red transition with an 80% colorimetric response at 3.0 mmol.L^{-1}, whereas NaDS did not alter the polymeric conformation and therefore did not cause a color change even at concentrations greater than 2.0 mmol.L^{-1}.

Our results for both vesicular suspensions show that the addition of the anionic surfactants NaDS or LiDS did not cause a significant colorimetric response, which was less than 5% in both cases. The repulsive force between the anionic surfactants and the negatively charged vesicles promoted repulsive interactions, and the result is almost no response. The anionic molecules caused a slightly stronger response in the presence of the co-solutes CHO and SPH than in pure PDA vesicles, suggesting that the presence of the cosolute decreases the repulsive interactions between the surfactant molecules and the polydiacetylenic matrix.

We performed microcalorimetric measurements to investigate the driving forces and the energy of the vesicle–surfactant interaction with the intention to confirm the mechanism proposed in the literature for vesicle–surfactant interactions. The energy associated with the consecutive addition of 9.2 × 10^{-10} mol of CTAB to 1.8 mL of an aqueous suspension of PDA or PDA/CHO/SPH was measured, and the results are presented in Figure 5. The concentration of the CTAB solution added to the vesicular suspensions was 10 times greater than the critical micellar concentration (c.m.c. = 9.2 × 10^{-3} mol.L^{-1}). Figure 5 shows the molar enthalpy change (ΔH_{obs}) as a function of the CTAB concentration. The ΔH_{obs} was measured when amphiphilic molecules were added to a vesicle suspension or to pure water (dilution enthalpy).

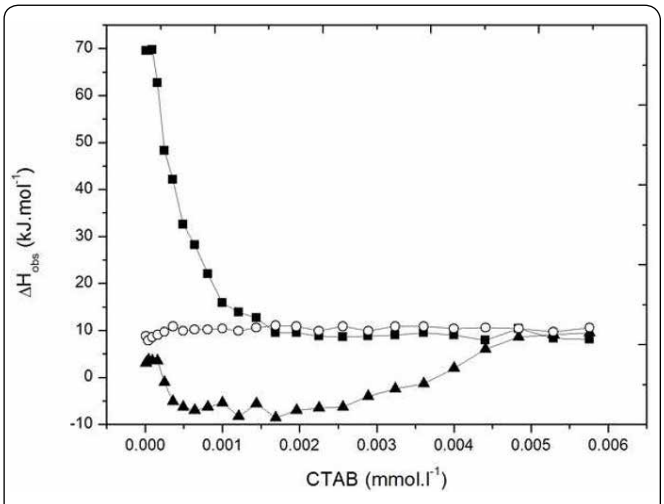

Figure 5: Molar enthalpy change (ΔH_{obs}) of increasing CTAB concentration added into (○) water, (■) PDA and (▲) PDA/CHO/SPH vesicles.

After aliquots of 9.2 x 10^{-10} mol of CTAB solution were added to 1.8 mL of pure water, the measured ΔH_{obs} values resulted from the following molecular processes: i) the dilution (ΔH_{dil}) and rupture (ΔH_{rup}) of the micelles; ii) the formation of the solution cavities that hold CTAB molecules (ΔH_{cav}); and iii) the solvation of CTAB molecules by water molecules (ΔH_{hid}). The positive ΔH_{obs} values indicate that more energy is absorbed by the first two processes than is released by the last one (Equation 2):

$$\Delta H_{w-obs} = \Delta H_{dil} + \Delta H_{rup} + \Delta H_{cav} + \Delta H_{hid} \quad .....(2)$$

This nearly constant absorbed energy ($\Delta H_{ves-obs}$ = + 10.0 kJ mol^{-1}) is attributed to the hydrophobicity of the surfactant, which makes its interaction with water molecules enthalpically unfavorable compared with the water–water interactions. The addition of CTAB to PDA or PDA/CHO/SPH suspensions promotes the same process described by Equation 2 in addition to the change in enthalpy associated with the CTAB–vesicle interaction (ΔH_{int}) (Equation 3):

$$\Delta H_{ves-obs} = \Delta H_{dil} + \Delta H_{rup} + \Delta H_{cav} + \Delta H_{hid} \quad .....(3)$$

When the same amount of CTAB was added to the PDA and the PDA/CHO/SPH suspensions, the change in the system enthalpy was dependent on the vesicles' composition, which demonstrated the effect of the co-solutes (CHO and SPH) on the vesicle–surfactant interaction. The enthalpy of the PDA suspension increased more than that of the water when the first aliquots of CTAB were titrated in the systems. However, the system enthalpy became lower compared to that of pure water when CTAB was added to the PDA/CHO/SPH vesicles. Interestingly, the abrupt change in ΔH_{Obs} occurred at range from 0 to 0.001 mmol.L^{-1} while the colorimetric transition occurred almost linear from 0 to 0.04 mmol.L^{-1}. The difference between ΔH_{Obs} and CR parameters demonstrated that different mechanisms were associated with colorimetric transition and with the determination of energy involved in vesicle-surfactant interaction. The first interaction step is the electrostatic interaction between CTAB and PDA, which occurred between 0 and 0.001 mmol.L^{-1}. Because this interaction is more energetic, it was determined by microcalorimeter. However, above this concentration further addition of CTAB promoted its insertion inside vesicle, whose energy could not be determined by the equipment.

In our experiment, the amount of surfactant that interacted with the vesicle could not be determined, which precluded determination of the absolute enthalpy of interaction. Therefore, we determined a thermodynamic parameter called the apparent molar interaction enthalpy (ΔH_{ap-int}), which was calculated by subtracting the energies involved in the process of CTAB addition to vesicles and to water (Equation 4):

$$\Delta H_{app-int} = \Delta H_{ves-obs} - \Delta H_{w-obs} \quad .....(4)$$

This parameter provides the apparent energy of the CTAB–vesicle interaction. Figure 6 shows ΔH_{ap-int} as a function of the CTAB concentration in the PDA and PDA/CHO/SPH suspensions.

The calorimetric data collected using a low surfactant concentration (1.03 × 10^{-4} mmol.L^{-1}) show that the PDA-CTAB interaction is entropically driven, whereas the PDA/CHO/SPH interaction involves an enthalpic contribution. These results show that there is a higher hydrophobic contribution for the PDA-CTAB interaction than for PDA/CHO/SPH interaction. The entropic contribution could be ascribed to two processes: i) the releasing of water molecules solvating the surfactant molecules and the hydrophilic surface of the vesicles, increasing the translational entropy of the system and ii) the conformational change associated with PDA molecules, which transform from a linear chain to a coil structure, increasing the conformational entropy of the vesicle [12], and/or twist out of planarity during the colorimetric transition, but still largely linear.

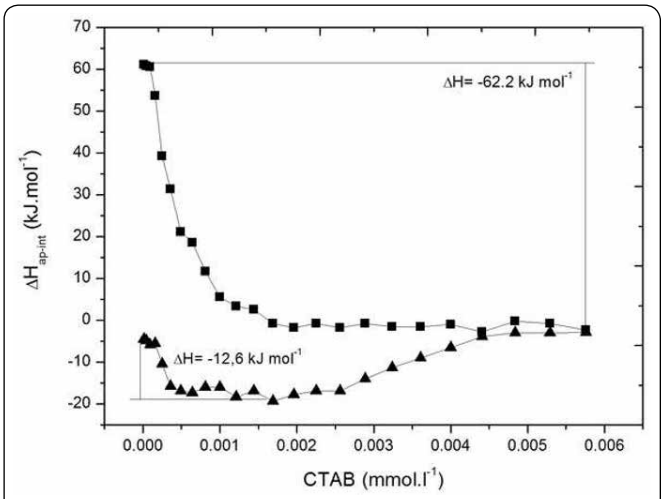

Figure 6: Apparent molar interaction enthalpy (ΔH_{ap-int}) of interaction between CTAB and (■) PDA and (▲) PDA/CHO/SPH suspensions as function of the CTAB concentration.

On the other hand, in the case of PDA/CHO/SPH vesicle, microcalorimetric results suggest that there is a specific enthalpic interaction between CTAB and cholesterol or CTAB and sphingomyelin, decreasing the system free energy by both enthalpy reduction and entropy enhance. Probably, these CTAB- cholesterol and CTAB-sphingomyelin interactions should be the cause of the poor colorimetric transition observed in the PDA/CHO/SPH vesicle.

For the titration of more than 0.03 µmol of CTAB (which corresponds to 1.20 × 10^{4} mmol.L^{-1}), the strong decrease in the absorbed energy, particularly for PDA vesicles, indicates that an cooperative thermodynamic process underlies the vesicle-surfactant interactions that is responsible for the energy release. Generally is thought that molecular conformation changes, such as side chain packaging, ordering and/or orientation changes, induce a stress in the polymer backbone, altering its π-π^* electronic state, which modifies its absorption and emission of visible light [15].

For PDA vesicles, the ΔH_{ap-int} started at + 62 kJ mol^{-1}, which indicates an initial hydrophobic contribution to the formation of the CTAB-PDA complex. As more CTAB was added, the ΔH_{ap-int} decreased and at a CTAB concentration of 0.005 mmol.l^{-1}, it remained constant at approximately zero, which indicated the end of the PDA-CTAB interactions. We consequently proposed that the difference between these both pathamar is the amount of energy associated with the colorimetric transition in the PDA vesicles induced by interaction with the CTAB molecules ($\Delta H_{ves-trans}$ = -62.2 kJ mol^{-1}). This amount of energy is too high to be attributed

only to conformational changes in the PDA chains, which suggests that other molecular processes, such as the insertion of the CTAB molecules inside of vesicle hydrophobic core, occur simultaneously. A possible mechanism is that cationic amphiphilic molecules adsorb at the vesicle surfaces, and the hydrophobic interactions result in reorientation of the surfactant molecules that inserted themselves into the hydrophobic domain of the vesicles. This CTAB insertion changes the PDA molecules' conformation, altering its backbone structure and consequently its π-π^* electronic state causing the colorimetric transition from the blue form to the red form [16].

The interaction between CTAB and PDA affects the dimensions of the nanostructures and causes the hydrodynamic radius (R_h) to increase by a factor of approximately 2.4. The R_h of the PDA vesicles, measured by DLS, was initially 39.82 ± 3 nm and increased to 96.85 ± 3 nm after the surfactants addition (3.8×10^{-5} mol.L^1 CTAB) and complete PDA conversion from blue to red structure. This size increase could be attributed to decreasing of polydiacetylenic backbone packaging caused by CTAB incorporation in hydrophobic core of PCDA aggregated.

The same profile of the $\Delta H_{ap\text{-}int}$ vs. [CTAB] curve obtained for the PDA-surfactant interactions was observed for the PDA/CHO/SPH vesicles. However, the change in enthalpy associated with the colorimetric transition in the PDA/CHO/SPH vesicles was lower than that observed for the PDA transition ($\Delta H_{ves\text{-}trans}$ = -12.6 kJ mol^{-1}). This result demonstrates the contribution of the cholesterol and sphingomyelin molecules to the vesicle stabilization increased, becoming less enthalpically favorable the blue-to-red transition.

As shown by the CR (%) vs. [CTAB] curves (Figures 3 and 4), a higher CR in the PDA vesicle than in the PDA/CHO/SPH system can be achieved with a small amount of CTAB, which suggests that a more favorable interaction occurs between the CTAB and the PDA vesicles. The microcalorimetric results demonstrated that these strong PDA-CTAB interactions was entropically driven.

The weaker PDA/CHO/SPH-CTAB interaction caused a smaller change in the vesicle size. The R_h of the PDA/CHO/SPH vesicles was 160.89 ± 3 nm and 219.84 ± 3 nm before and after the addition of CTAB. These results support the hypothesis that the mechanism of the blue-to-red transition is different in the presence of the CHO and SPH co-solutes. Probably there was a decrease in CTAB incorporation in PDA/CHO/SPH vesicles, decreasing PDA unpackaging and consequently reducing the vesicle expansion. This difference is likely related to the formation of microdomains of CHO and SPH, which create regions with different molecular packing's enthalpically stabilized [35].

As we have demonstrated previously, anionic surfactants induce a small colorimetric transition in PDA vesicles. We conducted microcalorimetric experiments on the mixture of vesicle suspensions and anionic surfactants aqueous solutions to measure the energy involved in the vesicle-NaDS and vesicle-LiDS interactions and to analyze the counterion (Na^+ or Li^+) contributions to such interactions. Figure 7 presents the enthalpy change observed during the titration of NaDS ($C_{12}H_{25}O_4SNa$) aqueous solution at 8.0×10^2 mol L^{-1} into vesicles and into pure water. The NaDS concentration was 10 times greater than the c.m.c.

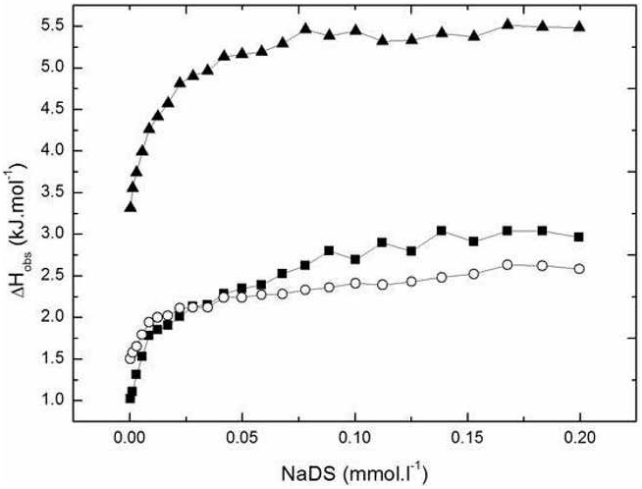

Figure 7: Molar enthalpy change (ΔH_{obs}) of increasing NaDS concentration added into (○) water, (■) PDA and (▲) PDA/CHO/SPH vesicles.

The mixtures of NaDS with pure water or vesicle aqueous suspensions were endothermic, and the ΔH_{obs} value increased with the amount of surfactant added. The dependence of ΔH_{obs} on the amount of NaDS added was almost coincident for the PDA vesicular suspension and pure water. A similar curve profile was observed for the titration of NaDS into PDA/CHO/SPH; however, the energy absorption was higher, which indicates that the CHO and SPH molecules influence the vesicle-NaDS interactions.

Figure 8 illustrates $\Delta H_{ap\text{-}int}$ as a function of the NaDS concentration, where $\Delta H_{ap\text{-}int}$ is calculated by subtracting the observed enthalpies after NaDS addition into water from NaDS addition into PDA or PDA/CHO/SPH vesicle suspension.

The results in Figure 8 indicate that a molecular interaction occurs between the vesicles and NaDS, i.e., $\Delta H_{ap\text{-}int}$ is not zero. However, because $\Delta H_{ap\text{-}int}$ value were so small such an interaction is not sufficient to promote a spectrophotometric transition of the nanostructures. This finding contradicts the conclusion of Su et al. [15], who attributed the absence of a colorimetric transition of PDA vesicles in the presence of anionic surfactants to the lack of an interaction between the chemical species. Both vesicular suspensions exhibited an increase in $\Delta H_{ap\text{-}int}$ as the concentration of NaDS was increased. The $\Delta H_{ap\text{-}int}$ varied from -0.5 to +0.5 kJ mol^{-1} for the interaction between NaDS and PDA and from +1.75 to +3.00 kJ mol^{-1} for the interaction between NaDS and PDA/CHO/SPH, which indicates that the vesicle-NaDS interaction is predominantly enthalpically unfavorable. We determined the R_h of the vesicles in the presence and absence of the surfactant. Without NaDS, the dimensions were 39.82 ± 3 nm for PDA and 160.89 ± 3 nm for PDA/CHO/SPH, and they increased to 43.50 ± 3 nm for PDA and 201.91 ± 3 nm for PDA/CHO/SPH after the addition of 8.90 mmol.l^{-1} of surfactant.

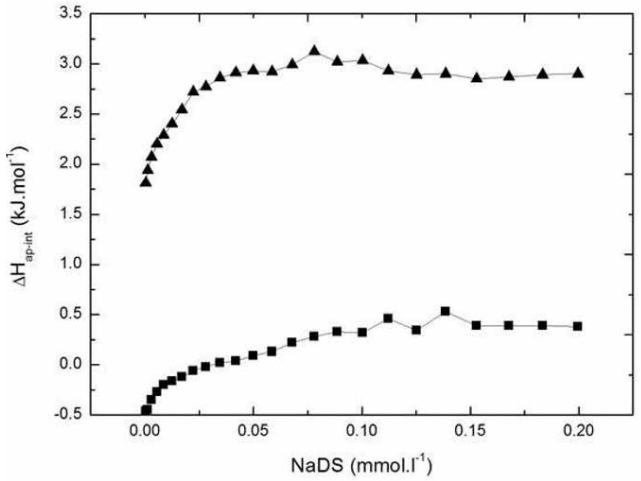

Figure 8: Apparent molar interaction enthalpy ($\Delta H_{ap\text{-}int}$) of interaction between NaDS and (■) PDA and (▲) PDA/CHO/SPH suspensions as function of the NaDS concentration.

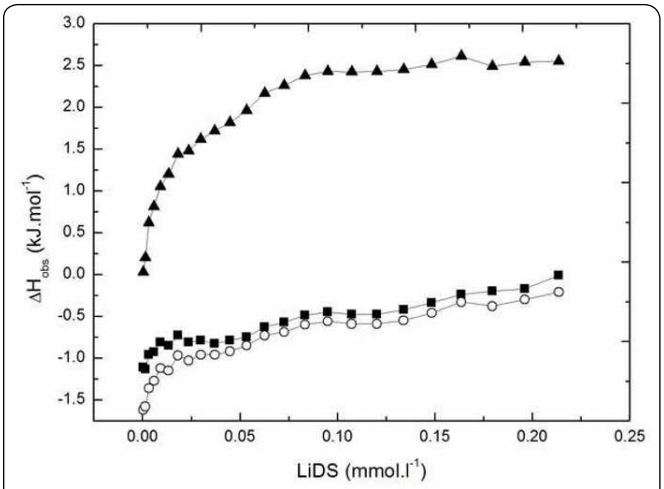

Figure 9: Molar enthalpy change (ΔHobs) of increasing LiDS concentration added into (○) water, (■) PDA and (▲) PDA/CHO/SPH vesicles.

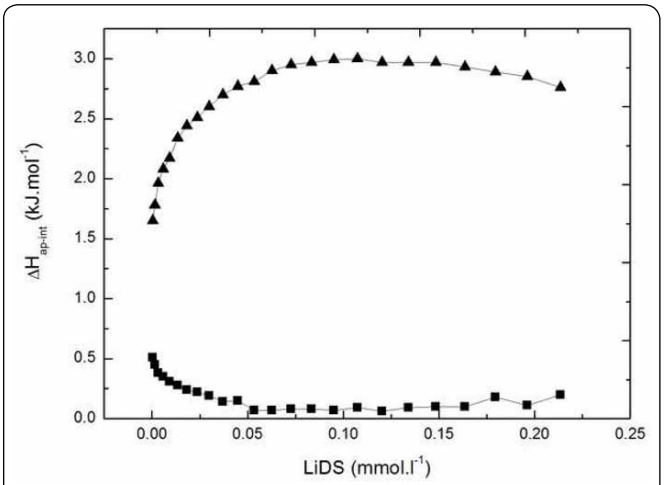

Figure 10: Apparent molar interaction enthalpy ($\Delta H_{ap\text{-}int}$) of interaction between LiDS and (■) PDA and (▲) PDA/CHO/SPH suspensions as function of the CTAB concentration.

To evaluate the effect of the surfactant counterion, additional microcalorimetric experiments were conducted with LiDS ($C_{12}H_{25}O_4SLi$) at a concentration of 8.6×10^{-2} mol L^{-1}, which is 10 times higher than the LiDS c.m.c. Figure 9 presents the results obtained for the titration of aliquots of 8.6×10^{-8} mol of LiDS into 1.8 mL of aqueous suspensions of PDA and PDA/CHO/SPH vesicles.

The results show that slightly more energy is released with the addition of LiDS into water and PDA vesicles compared with the addition of NaDS. In addition, it was possible to detect the effect of counterion since the titration of LiDS into pure PDA vesicles occurred with energy absorption while with NaDS there was energy release. However, the addition of LiDS to PDA/CHO/SPH absorbed almost the same energy as did the addition of NaDS, which indicates that the counterion plays an insignificant role in the interaction between the DS anion and the PDA/CHO/SPH aggregates. This small energetic difference between NaDS-vesicle and LiDS-vesicle interactions demonstrate that the main surfactant structure which interact with vesicle is the anion (CH_3-$(CH_2)_{11}$-SO_4^{2-}). Similar to NaDS, LiDS increased the size of the PDA and PDA/CHO/SPH vesicles by ΔR_h=3.93 ± 0.3 nm and 49.35 ± 1.5 nm, respectively. The larger growth of the PDA/CHO/SPH vesicles compared with that of the PDA vesicles corroborates our hypothesis that the presence of the co-solutes CHO and SPH modifies the interaction between the self-assembled structures of PDA/CHO/SPH and the surfactants. The interaction with NaDS and LiDS may induce a change in the PDA–CHO and/or PDA–SPH interactions and result in an expansion of the PDA/CHO/SPH vesicle.

The $\Delta H_{ap\text{-}int}$ between LiDS and PDA and that between LiDS and PDA/CHO/SPH were obtained by subtracting the ΔH_{obs} of the addition of surfactant to water from that of the addition of surfactant to the vesicles (Figure 10). For both vesicles, the transfer of the surfactant from the aqueous phase to the vesicle interior is enthalpically unfavorable because the interactions occur with energetic cost. As with the addition of NaDS, the addition of LiDS does not cause a colorimetric transition, which indicates that the interactions are not sufficiently strong to induce changes in the chain conformation of the polydiacetylenes.

Conclusions

The addition of a cationic surfactant (CTAB) induced a colorimetric transition in PDA and PDA/CHO/SPH vesicles; however, the presence of CHO and SPH molecules influenced the colorimetric transition mechanism.

The CTAB–vesicle interaction is entropically driven due to the release of solvation water molecules, which is possible mainly a result of CTAB insertion into the vesicle core. As indicated by the microcalorimetric results, the anionic surfactants interacted with the vesicles; however, the interaction was not sufficiently strong to change the chain conformation and cause a blue-to-red transition in either PDA or PDA/CHO/SPH vesicles.

The interaction between the anionic surfactants and the vesicles is mediated by the counterion, which likely reduces

the electrostatic repulsion between the negative charges of the vesicles and the surfactant heads. Polydiacetylene vesicles show potential to be used in sensors to detect cationic surfactants.

Acknowledgements

We gratefully acknowledge Conselho Nacional de Desenvolvimento Científico e Tecnológico (CNPq), Fundação de Amparo à Pesquisa do Estado de Minas Gerais (FAPEMIG) and Coordenação de Aperfeiçoamento de Pessoal de Nível Superior (CAPES) for their financial support of this project. J.P.R thanks CNPq for scholarships.

References

1. Li R, Kuda T, Yano T. 2014. Effect of food residues on efficiency of surfactant disinfectants against food related pathogens adhered on polystyrene and ceramic surfaces. *LWT-Food Sci Technol* 57(1): 200-206. doi: 10.1016/j.lwt.2013.11.018
2. Zaki HMBA, Mohamed HMH, El-Sherif AMA. 2015. Improving the antimicrobial efficacy of organic acids against *Salmonella enterica* attached to chicken skin using SDS acceptable sensory quality. *LWT-Food Sci Technol* 64(2): 558-564. doi:10.1016/j.lwt.2015.06.012
3. Koner S, Pal A, Adak A. 2011. Utilization of silica gel waste for adsorption of cationic surfactant and adsolubilization of organics from textile wastewater: a case study. *Desalination* 276(1): 142-147. doi: 10.1016/j.desal.2011.03.035
4. Kim KW, Choi H, Lee GS, Ahn DJ, Oh MK. 2008. Effect of phospholipid insertion on arrayed polydiacetylene biosensors. *Colloids Surf B Biointerfaces* 66(2): 213-217. doi: 10.1016/j.colsurfb.2008.06.020
5. Potisatityuenyong A, Rojanathanes R, Tumcharern G, Sukwattanasinitt M. 2008. Electronic absorption spectroscopy probed side-chain movement in chromic transitions of polydiacetylene vesicles. *Langmuir* 24(9): 4461-4463. doi: 10.1021/la800354q
6. Kamphan A, Traiphol N, Traiphol R. 2016. Versatile route to prepare reversible thermochromic polydiacetylene nanocomposite using low molecular weight poly (vinylpyrrolidone) *Colloids Surface A* 497: 370-377. doi: 10.1016/j.colsurfa.2016.03.041
7. Cheng Q, Stevens RC. 1998. Charge-induced chromatic transition of amino acid-derivatized polydiacetylene liposomes. *Langmuir* 14(8): 1974-1976. doi: 10.1021/la980185b
8. Yuan Z, Hanks TWA. 2008. A reversible colorimetric and fluorescent polydiacetylene vesicle sensor platform. *Polymer* 49(23): 5023-5026. doi: 10.1016/j.polymer.2008.09.008
9. Nallicheri RA, Rubner MF. 1991. Investigations of the mechanochromic behavior of poly (urethane-diacetylene) segmented copolymers. *Macromolecules* 24(2): 517-525. doi: 10.1021/ma00002a027
10. Lee SS, Chae EH, Ahn DJ, Ahn KH, Yeo JK. 2007. Shear-induced color transition of PDA (polydiacetylene) liposome in polymeric solutions. *Korea-Aust Rheol J* 19(1): 43-47.
11. Chance RR. 1980. Chromism in polydiacetylene solutions and crystals. *Macromolecules* 13(2): 396-398. doi: 10.1021/ma60074a037
12. Pires ACS, Soares NFF, da Silva LHM, da Silva MCH, Mageste AB, et al. 2010. Thermodynamic study of colorimetric transitions in polydiacetylene vesicles induced by the solvent effect. *J Phys Chem B* 114(42): 13365-13371. doi: 10.1021/jp105604t
13. Lee S, Cheng H, Chi M, Xu Q, Chen X, et al. 2016. Sensing and antibacterial activity of imidazolium-based conjugated polydiacetylenes. *Biosens Bioelectron* 77: 1016-1019. doi: 10.1016/j.bios.2015.10.090
14. Nopwinyuwong A, Kitaoka T, Boonsupthip W, Pechyen C, Suppakul P. 2014. Effect of cationic surfactants on characteristics and colorimetric behavior of polydiacetylene/silica nanocomposites as time-temperature indicator. *Appl Surf Sci* 314: 426-432. doi: 10.1016/j.apsusc.2014.07.013
15. Su YL, Li JR, Jiang L. 2004. Effect of amphiphilic molecules upon chromatic transitions of polydiacetylene vesicles in aqueous solutions. *Colloids Surf B Biointerfaces* 39(3): 113-118. doi: 10.1016/j.colsurfb.2003.12.005
16. Song J, Cheng Q, Kopta S, Stevens RC. 2001. Modulating artificial membrane morphology: pH-induced chromatic transition and nanostructural transformation of a bolaamphiphilic conjugated polymer from blue helical ribbons to red nanofibers. *J Am Chem Soc* 123(14): 3205-3213. doi: 10.1021/ja0035046
17. Su YL, Li JR, Jiang L. 2005. A study on the interactions of surfactants with phospholipid/polydiacetylene vesicles in aqueous solutions. *Colloids Surface A* 257-258: 25-30. doi: 10.1016/j.colsurfa.2004.10.058
18. Silbert L, Shlush IB, Israel E, Porgador A, Kolusheva S, et al. 2006. Rapid chromatic detection of bacteria by use of a new biomimetic polymer sensor. *Appl Environ Microbiol* 72(11): 7339-7344. doi: 10.1128/AEM.01324-06
19. Jung YK, Kim TW, Jung C, Cho DY, Park HG. 2008. A polydiacetylene microchip based on a biotin-streptavidin interaction for the diagnosis of pathogen infections. *Small* 4(10): 1778-1784. doi: 10.1002/smll.200800947
20. Su YL, Li JR, Jiang L. 2004. Chromatic immunoassay based on polydiacetylene vesicles. *Colloids Surf B Biointerfaces* 38(1-2): 29-33. doi: 10.1016/j.colsurfb.2004.08.010
21. Su YL, Li JR, Jiang L, Cao J. 2005. Biosensor signal amplification of vesicles functionalized with glycolipid for colorimetric detection of *Escherichia coli*. *J Colloid Interface Sci* 284(1): 114-119. doi: 10.1016/j.jcis.2004.10.003
22. Souza LC, Rezende JP, Pires ACS, Silva LHM, Silva MCH, et al. 2016. Polydiacetylene/triblock copolymer nanoblend applied as a sensor for micellar casein: a thermodynamic approach. *Food Chem* 197(PtA): 841-847. doi: 10.1016/j.foodchem.2015.11.071
23. Jung YK, Park HG, Kim JM. 2006. Polydiacetylene (PDA)-based colorimetric detection of biotin-streptavidin interactions. *Biosens Bioelesctron* 21(8): 1536-1544. doi: 10.1016/j.bios.2005.07.010
24. Ma G, Cheng Q. 2006. Manipulating FRET with polymeric vesicles: development of a "mix-and-detect" type fluorescence sensor for bacterial toxin. *Langmuir* 22(16): 6743-6745. doi: 10.1021/la0613070
25. Pevzner A, Kolusheva S, Orynbayeva Z, Jelinek R. 2008. Giant chromatic lipid/polydiacetylene vesicles for detection and visualization of membrane interactions. *Adv Funct Mater* 18(2): 242-247. doi: 10.1002/adfm.200700726
26. Charych DH, Nagy JO, Spevak W, Bednarski MD. 1993. Direct colorimetric detection of a receptor-ligant interaction by a polymerized bilayer assembly. *Science* 261(5121): 585-588. doi: 10.1126/science.8342021
27. Mageste AB, Santos JB, Ferreira GMD, da Silva MCH, Teixeira AVNC, et al. 2010. Microcalorimetric and SAXS determination of PEO-SDS interactions: the effect of co-solutes formed by ions. *J Phys Chem* 114(37): 11967-11974. doi: 10.1021/jp1032178
28. Boullanger P, Lafont D, Bouchu MN, Jiang L, Liu T, et al. 2008. The use of glycolipids inserted in color-changeable polydiacetylene vesicles, as targets for biological recognition. *C R CHIM* 11(1-2): 43-60. doi: 10.1016/j.crci.2007.03.007
29. Sun C, Zhang Y, Fan Y, Li Y, Li J. 2004. Mannose-*Escherichia coli* interaction in the presence of metal cations studied *in vitro* by colorimetric polydiacetylene/glycolipid liposomes. *J Inorg Biochem* 98(6): 925-930. doi: 10.1016/j.jinorgbio.2004.03.006
30. Rozner S, Kolusheva S, Cohen Z, Dowhan W, Eichler J, et al. 2003. Detection and analysis of membrane interactions by a biomimetic colorimetric lipid/polydiacetylene assay. *Anal Biochem* 319(1): 96-104. doi: 10.1016/S0003-2697(03)00278-1
31. Groysman N, Orynbayeva Z, Katz M, Kolusheva S, Khanin M, et al. 2008. Membrane processes and biophysical characterization of living cells decorated with chromatic polydiacetylene vesicles. *Biochim Biophys*

Acta 1778(5): 1335-1343. doi: 10.1016/j.bbamem.2008.01.028

32. Brown DA, London E. 2000. Structure and function of sphingolipid- and cholesterol-rich membrane rafts. *J Biol Chem* 275(23): 17221-17224. doi: 10.1074/jbc.R000005200
33. Massey JB. 2001. Interaction of ceramides with phosphatidylcholine, sphingomyelin and sphingomyelin/cholesterol bilayers. *Biochim Biophys Acta* 1510(1-2): 167-184. doi: 10.1016/S0005-2736(00)00344-8
34. Holopainen JM, Metso AJ, Mattila JP, Jutila A, Kinnunen PKJ. 2004. Evidence for the lack of a specific interaction between cholesterol and sphingomyelin. *Biophys J* 86(3): 1510-1520. doi: 10.1016/S0006-3495(04)74219-8
35. Sheynis T, Jelinek R. 2010. Lipid-induced calcitonin fibrillation blocks membrane interactions of a peptide antibiotic. *J Phys Chem B* 114(47): 15530-15535. doi: 10.1021/jp1072473